### Title

The role of small heterodimer partner in nonalcoholic fatty liver disease improvement after sleeve gastrectomy in mice




### Journal

Obesity, 22(11)

### ISSN

1930-7381



### Authors

Myronovych, Andriy
Salazar-Gonzales, Rosa-Maria
Ryan, Karen K
et al.



### Publication Date

2014-11-01

### DOI

10.1002/oby.20890

Peer reviewed

HHS Public Access

Author manuscript

*Obesity (Silver Spring)*. Author manuscript; available in PMC 2015 November 01.

Published in final edited form as:

*Obesity (Silver Spring)*. 2014 November ; 22(11): 2301–2311. doi:10.1002/oby.20890.

# The Role of Small Heterodimer Partner (SHP) in NAFLD Improvement after Vertical Sleeve Gastrectomy in Mice

**Andriy Myronovych, MD, PhD**[1], **Rosa-Maria Salazar-Gonzales, PhD**[1], **Karen K. Ryan, PhD**[3], **Lili Miles, MD**[1], **Wujuan Zhang, PhD**[2], **Pinky Jha, MS**[2], **Li Wang, PhD**[4], **Kenneth DR Setchell, PhD**[2], **Randy J Seeley, PhD**[3], and **Rohit Kohli, MBBS, MS**[1,3]

[1]Department of Pediatrics, Division of Gastroenterology, Hepatology and Nutrition, Cincinnati Children's Hospital Medical Center, 3333 Burnet Avenue, Cincinnati, Ohio, USA

[2]Department of Pathology and Laboratory Medicine, Cincinnati Children's Hospital Medical Center, 3333 Burnet Avenue, Cincinnati, Ohio, USA

[3]Metabolic Diseases Institute, Department of Internal Medicine, University of Cincinnati College of Medicine, 2170 E. Galbraith Road, Cincinnati, Ohio, USA

[4]Departments of Medicine and Oncological Sciences, Huntsman Cancer Institute, University of Utah School of Medicine, 30 North 1900 East SOM 4R118, Salt Lake City, Utah, USA

## Abstract

**Objective—**Bile acids (BA) are elevated after vertical sleeve gastrectomy (VSG) and farnesoid-X-receptor (FXR) is critical to the success of murine VSG. BA down-regulate hepatic lipogenesis by activating the FXR-small heterodimer partner (SHP) pathway. We tested the role of SHP in fatty liver disease (NAFLD) improvement after VSG.

**Design and Methods—**Wild type (WT), SHP liver-transgenic (SHP-Tg) and SHP knockout (SHP-KO) high-fat diet (HFD) fed mice underwent either VSG or Sham surgery. Body weight, BA level & composition, steatosis and BA metabolism gene expression were evaluated.

**Results—**Obese WT mice post-VSG lost weight, reduced steatosis, decreased plasma alanine aminotransferase (ALT), had more BA absorptive ileal area, and elevated serum BA. Obese SHP-Tg mice post-VSG also lost weight and had decreased steatosis. SHP-KO mice were however resistant to steatosis despite weight gain on a HFD. Further SHP-KO mice that underwent VSG lost weight but developed hepatic inflammation and had increased ALT.



**Corresponding author contact information:** Rohit Kohli, MBBS, MS, Department of Pediatrics, Division of Gastroenterology, Hepatology and Nutrition, Cincinnati Children's Hospital Medical Center, MLC 2010, 3333 Burnet Avenue, Cincinnati, Ohio, USA, 45229. Tel.: 1-513-803-0908, Fax: 1-513-803-2785, rohit.kohli@cchmc.org.

**Conflicts of Interest Statement:**
The other coauthors have no disclosures.

**Author Contributions:**
AM, RMSG, and RK conceived and carried out experiments, LM, KKR, KDRS, LW, and RJS conceived experiments and analyzed data. WZ, PJ carried out experiments. All authors were involved in writing the manuscript and had final approval of the submitted and published versions.

**Conclusions—**VSG produces weight loss independent of SHP status. SHP ablation creates a pro-inflammatory phenotype which is exacerbated after VSG despite weight loss. These inflammatory alterations are possibly related to factors extrinsic to a direct manifestation of NASH.

### Keywords

Bile acid metabolism; bariatric surgery; obesity; inflammation

## Introduction

NAFLD (nonalcoholic fatty liver disease) is the hepatic complication of obesity, the pathognomonic characteristic of which is liver lipid accumulation (1). The severe form of this disease is nonalcoholic steatohepatitis (NASH) that can progress to cirrhosis (2). Bariatric surgery is the most effective treatment for morbid obesity and its comorbidities including NASH (3). In addition to weight loss and its direct metabolic benefits, bariatric surgery causes weight-loss independent metabolic improvements (4). We have previously reported that one such benefit is hepatic steatosis reduction. We observed that diet-induced obese mice that underwent vertical sleeve gastrectomy (VSG), had less hepatic lipid accumulation than body-weight and food-intake matched mice that underwent Sham operations (5).

Our work attempts to understand the mechanism by which hepatic steatosis reduction occurs after VSG. One such clue may be the fact that patients have elevated serum bile acid (BA) levels following bariatric surgery, including VSG (6, 7). We observed a similar increase in serum BA in obese mice subjected to VSG (5). A large body of evidence suggests that circulating BA act as signaling molecules, which through transcription factor farnesoid-X-receptor (FXR) and other receptors are able to regulate their own synthesis and multiple energy metabolism pathways (8). However, it remains unknown whether the *weight-loss independent* benefit of hepatic steatosis reduction is due to changes in BA physiology or BA triggered signaling. Using FXR-knockout mice we recently reported that in the absence of FXR, the ability of VSG to reduce body weight and improve glucose tolerance was substantially reduced, further pointing to the importance of the BA signaled FXR pathway in metabolic improvements observed after VSG (9). Small heterodimer partner (SHP) is an atypical orphan nuclear receptor that is directly influenced by FXR and regulates several processes in the liver, including BA, lipid, glucose homeostasis and immune responses (10, 11),(12). SHP-knockout (SHP-KO) mice demonstrate increased BA pool size compared to their wild type (WT) littermates. On a chow diet hepatic triglyceride levels are not different between the groups. However, after the administration of diet rich in cholic acid (CA) triglyceride levels are reduced in WT but not in SHP-KO (13). Therefore, SHP-KO mice are unresponsive to the lipid reducing effect of CA. BA in general and CA in particular are increased after VSG (5), which points to the importance of BA-FXR-SHP pathway for the hepatic steatosis reduction after VSG. We therefore, aimed to dissect the signaling mechanism(s) activated in response to VSG focusing on the importance of SHP for the hepatic improvements seen after VSG in obese mice.

We hypothesized that SHP activation by BA is necessary for the hepatic steatosis improvement observed after VSG. VSG was performed in diet-induced obese mice with either hepatocyte overexpression of SHP (SHP-Tg) or SHP deletion (14). We found that both SHP-Tg and SHPKO mice gained weight on a high fat diet (HFD) and VSG resulted in weight loss in both strains. SHP-Tg mice developed steatosis on a HFD that was reduced after VSG but SHP-KO mice were resistant to HFD-induced hepatic steatosis. Further SHP-KO mice on the HFD had a pro-inflammatory hepatic phenotype that exacerbated despite weight loss post-VSG. Thus, we conclude that an intact SHP signaling pathway is important for the inflammation prevention after VSG.

## Methods

### Animals and Diets

Studies were approved by the Institutional Animal Care and Use Committee at Cincinnati Children's Hospital Medical Center. For the BA intestinal composition study male C57Bl/6 mice were purchased from the Jackson laboratory, Bar Harbor, ME. Other data from this experiment had been published in our previous study (5). SHP-Tg and SHP-KO mice on C57Bl/6 background were backcrossed with the WT and obtained heterozygous mice were used for the establishing of colony. Mice were housed in a temperature controlled room (22±2°C) on a 12 hour light-dark cycle. To induce obesity male six week-old mice received 60 kcal% saturated HFD (Research Diets, New Brunswick, NJ) for 6 weeks before surgery in case of SHP-Tg experiment and for 8 weeks in case of the SHP-KO study as SHP-KO mice gained weight at a slower pace. In phenotype SHP-Tg and SHP-KO studies mice did not receive any surgeries and were on a HFD until sacrifice. Two groups were present in each phenotype study, viz. SHP-Tg (or SHP-KO) and WT. Mice had ad libitum diet access except Sham pair fed (Sham-PF) mice which received an average amount of food consumed by the VSG group the day before.

### Surgery and Post-operative Care

Surgeries and post-operational care were performed as previously described (5). In case of SHP-Tg VSG study, mice were randomized into four groups: SHP-Tg mice which underwent Sham surgery and SHP-Tg mice which were subjected to the VSG; their WT littermates similarly received Sham or VSG surgery. The same grouping paradigm was used in case of SHP-KO VSG experiment. Body weight and food intake were measured at fixed intervals. Blood for serum samples preparation was collected by tail vein bleeding after four-hour fasting period at 7 days prior to and 14, 28, 42 and 56 days post-surgery. All mice were sacrificed in a postprandial condition at day 60 post-surgery. Mice were fasted overnight and then one hour before sacrifice 0.5 ml of liquid diet Osmolite (Abbott Laboratories, Columbus, OH) was administered by oral gavage to each mouse. Serum and liver samples were collected at time of sacrifice, performed between 10:00 a.m. and 1:00 p.m. taking into account diurnal variation of some genes' expression. Liver aliquots were snap-frozen, fixed in 10% formalin for histology or used fresh for the flow cytometry.

### Body Composition Analysis

Using Echo MRI Whole Body Composition Analyzer (Echo Medical Systems, Houston, Texas) fat mass of Sham and VSG mice was evaluated prior to and at day 49 post-surgery as previously described (5).

### Glucose Quantification

Blood samples collected by the tail bleeding at day 14 post-surgery after four-hour fasting period were utilized. One Touch Glucometer (LifeScan, Milpitas, CA) was utilized.

### Hepatic Triglyceride, Alanine Aminotransferase (ALT), Bilirubin, BA Quantification, BA Serum and Intestinal Composition Analyses

Triglyceride quantification: 100 mg of liver was homogenized in 1 ml of 20 mM Tris buffer and analyzed by Triglycerides Reagent Set. Serum bilirubin was quantified by Total Bilirubin Reagent Set. Both sets were purchased from Pointe Scientific, Canton, MI. Plasma ALT: Kinetic absorbance was measured at 340 nm using Discret Pak™ ALT Reagent Kit (Catachem, Bridgeport, CT). BA were measured by Total Bile Acids Assay Kit (Bio-Quant, San Diego, CA). Assays were performed per manufacturers' protocols. Serum and intestinal BA composition and quantification were assayed using electro-spray ionization liquid chromatography mass spectrometry (ESI-LC-MS) as previously described (15).

### Histology

Hematoxylin & eosin stained sections were prepared in the Histology Core of our Digestive Disease Research Center. Images were obtained by Olympus BX51TF microscope (Olympus Corporation, Tokyo, Japan). Apical sodium-dependent bile acid transporter protein (ASBT) expression in the terminal ileum was assessed by immunofluorescence. Sections were incubated with anti-ASBT antibody (Santa Cruz Biotechnology, Dallas, TX) and positively stained area was measured using Image-Pro® Plus software (Media Cybernetics, Bethesda, MD).

### qPCR Gene Expression Evaluation

cDNA was prepared using TaqMan™ Reverse Transcription kit and protocol (Applied Biosystems, Carlsbad, CA). Reactions were accomplished in an Eppendorf Mastercycler (Eppendorf, Hamburg, Germany). Relative mRNA expression was evaluated by the FAM real-time kinetic PCR on a Stratagene Mx-3005 Multiplex Quantitative PCR Machine (Stratagene, Agilent Technologies, La Jolla, CA). Ribosomal 18S gene was used as a standard and standard curve method was applied to calculate expression. TaqMan™ primers were utilized (Applied Biosystems, Carlsbad, CA).

### Flow Cytometry

Liver immune cells were isolated using the Gentlemacs Dissociator (Miltenyi Biotec Inc., San Diego, CA) and Percoll gradient. Flow cytometry of liver immunocompetent cells was performed. Cells were stained using fluorescent labeled specific antibodies (eBioscience Inc., San Diego, CA), CD3, CD4, CD8, NK1.1 and CD69. (Figure S1).

### Statistical Analysis

All values are expressed as mean ± SEM. Statistical significance was evaluated by one- or two-way ANOVA and, where indicated, Student's t-test to compare two groups. *P* values less than 0.05 were considered to be significant. Serum BA composition data was not normally distributed and therefore expressed as log transformed.

## Results

Two groups of HFD induced obese mice were subjected to either VSG or Sham surgery with food restriction (pair feeding) to that of VSG mice (Sham-PF). At day 60 post-surgery no difference was observed in body weight between two groups (34.30±1.34 g VSG vs. 35.78±1.3 g Sham-PF). However, VSG mice exhibited longer villi (348.2±4.95 μm vs. 268.2±6.06 μm) with greater surface area (14.28±1.12 $mm^2$ vs. 10.19±1.12 $mm^2$) (Figure 1A) and more ASBT staining in the terminal ileum compared to Sham-PF mice (400.3±86.63 $\mu m^2$ vs. 159.8±29.41 $\mu m^2$) (Figure 1B). Described changes were observed only in the ileum of VSG mice, while no morphological changes were visible in the jejunum. BA composition in the intestines of VSG mice was different than in the Sham-PF mice, with increased unconjugated BA in the jejunum and decreased conjugated BA in the ileum compared to the Sham-PF group (Figure 1C). We further observed that levels of unconjugated muricholic, cholic, ursodeoxycholic, hyodeoxycholic, chenodeoxycholic and deoxycholic acids were higher in the jejunum of VSG mice compared to Sham-PF mice. No such difference was observed in the ileum between the two groups, moreover, taurine-conjugated BA levels were even higher in the ileum of Sham-PF mice (Figure 1D). Together, these data point to the increased reabsorption of BA potentially via increased ASBT activity in the ileum of VSG mice.

SHP-Tg mice and their WT littermates were kept on HFD for 6 weeks, then randomized to Sham or VSG. Body weight, fat content and serum fasting BA levels pre-surgery were not different between genetically modified and WT mice (data not shown). SHP-Tg and WT mice post-VSG lost similar amount of body weight and had reduced food intake during the first week postsurgery (Figure 2A and B). Body fat was reduced similarly in both VSG groups (Figure 2C). Fasting serum BA levels were increased in WT VSG group at four weeks post-surgery (30.31±3.38 μmol/L) but this increase was not observed in SHP-Tg VSG mice (Figure 3A). However, when challenged with a postprandial condition on day 60 post-surgery serum BA levels were increased in SHP-Tg VSG group as well. Serum BA composition analysis showed that most unconjugated and taurine-conjugated BA levels were increased in SHP-Tg VSG mice (Figure 3B), similarly to that of WT mice post-VSG (Figure S2). BA synthesis and uptake gene expression was down-regulated in both VSG groups compared to Sham groups (Figure 3C and 3D). SHP-Tg mice after VSG do not exhibit increased fasting serum BA but after the postprandial challenge their BA metabolism characteristics are similar to that of WT mice.

The livers of both SHP-Tg and WT Sham mice had more lipid accumulation and higher triglyceride content compared to the livers of SHP-Tg and WT VSG mice (Figure 4A and 4B). Liver steatosis score was higher in both Sham groups (Figure 4C). Plasma ALT levels were the highest in WT Sham mice (232.6±63.92 IU/L) and were lower in WT VSG

(59.93±8.62 IU/L) and SHP-Tg VSG mice (52.89±8.0 IU/L) (Figure 4D). SHP-Tg mice, similar to WT VSG mice, have improved hepatic steatosis after VSG.

After 8 weeks on HFD SHP-KO mice and their WT littermates were subjected to either Sham or VSG surgery. SHP-KO mice were obese (34.39±0.7 g) but lighter in their pre-surgery body weight compared to WT mice (41.30±1.24 g, p= < 0.0001). Despite this initial difference in body weight SHP-KO and WT mice behaved similarly in terms of body weight lost/gained post-VSG (Figure 5A). VSG groups consumed less food during first two weeks post-surgery compared to Sham groups (Figure 5B). WT VSG and SHP-KO VSG mice had much less body fat (28.92±4.93 % and 16.94±1.88 %, respectively) compared to their respective WT Sham and SHP-KO Sham mice (39.67±0.84 % and 36.96±2.04 %) (Figure 5C). However, while fasting serum glucose levels were dramatically improved in WT VSG compared to WT Sham mice (129.6±3.31 mg/dL vs. 217.8±6.0 mg/dL) this was not observed between SHP-KO VSG and SHP-KO Sham mice (149.5±7.09 mg/dL vs. 182.3±14.07 mg/dL) (Figure 5D).

Fasting serum BA levels trended to be higher in SHP-KO compared to WT mice pre-surgery (38.10±2.55 μmol/L vs. 34.47±4.7 μmol/L, data not shown). Serum BA levels were increased in both WT and SHP-KO groups post-VSG (Figure 6A). Serum BA composition was assessed and, similarly to SHP-Tg VSG experiment, most individual unconjugated and taurine-conjugated BA, and as a result total BA levels were statistically higher in SHP-KO VSG compared to SHP-KO Sham mice 60 days post-surgery (Figure 6B). Total bilirubin levels were not different between the groups (data not shown). As expected, BA synthesis genes Cyp7a1 and Cyp8b1 were highly induced in SHP-KO Sham vs. WT Sham mice. Cyp8b1 was down-regulated in both VSG groups. Similarly VSG mice had down-regulated hepatic BA uptake genes, (Ntcp, Oatp2 and Oatp4), although Ntcp was expressed at variable levels in SHP-KO Sham and WT Sham groups (Figure 6C and 6D). SHP-KO mice gain weight and have a similar increase in serum BA levels and changes in BA metabolism post-VSG as WT mice.

Histological examination revealed increased lipid droplet accumulation in the livers of WT Sham group, while the microstructure of WT VSG mice was normal. SHP-KO Sham and SHP-KO VSG mice did not exhibit fat accumulation. Neutrophil infiltration was observed only in the livers of the SHP-KO VSG mice after surgery (Figure 7A). Similar to previous observations (16),(17) hepatic triglyceride content was lower in SHP-KO Sham vs. WT Sham mice. Triglyceride levels were dramatically reduced in WT VSG (4.26±0.71 mg per 100 mg wet liver) vs. WT Sham mice (32.92±6.22 mg), however, they were not further reduced in SHP-KO VSG vs. SHP-KO Sham mice (5.25±1.33 mg and 7.345±0.59 mg, respectively) (Figure 7B). Liver steatosis score mirrored triglyceride levels (Figure 7C). Plasma ALT levels were lower in WT mice after VSG (54.86±4.9 IU/L WT VSG vs. 113.7±17.47 IU/L WT Sham), but were not decreased in SHP-KO mice after VSG (99.60±10.23 IU/L SHP-KO VSG vs. 102.6±1.95 IU/L SHP-KO Sham) (Figure 7D). Unlike WT, SHP-KO mice develop hepatic inflammation after VSG.

## Discussion

Bariatric surgery in general and specifically our murine VSG model result in increased serum BA levels after surgery. We have identified that the BA responsive nuclear receptor FXR is a metabolic target responsible for positive outcomes after murine VSG (9). We have further observed a concomitant suppression of BA synthesis (Cyp7a1 and Cyp8b1) and BA uptake genes (Ntcp, Oatp) that is known to be caused by FXR activation (5). Recently obese patients with NAFLD were reported to have increased expression of Cyp7a1 and Ntcp indicating failure to activate SHP upon FXR stimulation (18). As SHP is known to directly modulate hepatic lipogenesis and gluconeogenesis (12) we proposed to determine the role of SHP in NAFLD improvements seen after VSG. We found that both SHP-Tg and SHP-KO mice lose weight after VSG however, hepatic inflammation developed in SHP-KO mice despite weight loss. Further fasting BA were not elevated in SHP-Tg mice after VSG. This can be explained by the signaling effect of SHP on BA synthesis, as its constant overexpression causes suppression of BA production genes Cyp7a1, Cyp8b1 and Cyp27a1 (19). However, this suppressive effect of SHP was apparently not sufficient in a postprandial state wherein we did observe an increase in serum BA.

### What are the consequences of elevated BA after VSG on FXR-SHP signaling in the hepatocyte?

A negative feedback loop wherein BA bind to FXR and induce SHP to suppress BA synthesis is well-recognized (20). SHP-KO mice show resistance to diet-induced obesity due to the increased basal expression of a dominant regulator of energy metabolism PGC-1α in brown adipocytes and increased energy expenditure (17). Unfortunately, the impact of SHP on hepatic fat metabolism is somewhat controversial. Certain reports suggest that SHP lowers triglyceride levels via downregulation of Srebp-1c when stimulated by CA (21) while hepatic steatosis and Srebp-1c expression are increased in SHP-KO compared to WT mice when treated with CA (13). Our data show that serum CA levels are increased post-VSG (5). Other studies describe that SHP-deficient mice have reduced hepatic triglyceride content as SHP negatively modulates hepatic lipid export, uptake, and synthesis (16, 22). Additionally, Boulias et al. showed that sustained expression of SHP leads to the depletion of hepatic BA pool and a concomitant accumulation of liver triglycerides (19).

Consistent with previous reports, in our study SHP-KO mice gained less weight than WT, however, they were still obese. SHP-KO mice being lighter, with less body fat and higher serum BA levels, did not show either improvement or impairment of hepatic triglyceride accumulation post-VSG. Further, SHP appears to take part in the systemic inflammatory response (23) as SHP-deficient mice are more susceptible to endotoxin-induced sepsis (24). Using flow cytometry analysis performed on the livers of WT and SHP-KO HFD-fed mice we observed that the ratios of T lymphocyte CD4-CD69+, CD8-CD69+ and NK-CD69+ immune cells were higher in the SHP-KO compared to the WT mice (Figure S3) pointing to the SHP-KO mice pro-inflammatory phenotype. Under the excess stress conditions, which are VSG and chronic HFD administration, it is possible that the pro-inflammatory phenotype would be exacerbated in SHP-KO mice. Indeed, hepatic inflammation developed in SHP-KO mice despite weight loss after VSG. Also plasma ALT levels were not reduced in SHP-

KO VSG mice. A key limitation of our study is that the experiments involving SHP-KO mice as designed did not facilitate complete evaluation of the inter-play of NAFLD and inflammation. SHP-KO mice did not develop histological NAFLD/NASH on a HFD and therefore we are unable to draw conclusions regarding the impact of VSG on NAFLD elements, including hepatic steatosis, from these specific experiments. We however do note that SHP plays a role in control of hepatic inflammation overall and that the lack of SHP signaling averts VSG, despite producing weight loss, from resulting in prevention of hepatic inflammation. Taken together these data suggest that having an intact SHP is necessary for the prevention of liver inflammation and injury seen after VSG in SHP-KO obese mice.

On the other hand, immune cell subpopulations were not different in the SHP-Tg compared to the WT mice (Figure S4). In contrast, SHP-Tg VSG mice did not show increased fasting serum BA but we observed similar reduction of hepatic steatosis as that of WT VSG mice. Deletion or overexpression of SHP exert neither positive nor negative effects on murine fatty liver disease post-VSG as the expression of Srebp-1c was not altered in these mice (data not shown).

### So why are serum BA elevated after VSG in the first place?

BA reabsorption in the terminal ileum occurs in an active manner against its concentration gradient (25) predominantly through the ASBT (26). Increased villi length and total surface area in addition to the greater ASBT stained area which were observed post-VSG potentially explain the elevated serum BA levels. This intestinal adaptive response is similar to that seen in other experimental bariatric and non-surgical murine cohorts that have been shown to have higher serum BA levels (5, 27, 28, 29, 30, 31). This increased BA absorption coupled with the suppression of hepatocyte BA uptake mechanisms (Oatp/Ntcp) may together result in elevated serum BA levels. Indeed similar suppression of BA uptake has been used to explain elevated serum BA by Vos et al. in a rat model of cholestasis (32). However, BA synthesis and uptake machinery were inhibited in all our mice post-VSG, pointing that this may be a SHP independent effect of VSG.

A limitation of our study is that the experiments involving SHP-KO and SHP-Tg mice did not have weight matched Sham control groups. Thus, we are unable to draw conclusions regarding weight-loss independent effects, including hepatic steatosis, from these specific cohorts. Additionally, our present study is not comprehensive by far. We focused on hepatic FXR-SHP axis, however, another enterohepatic BA signaling pathway comprised of fibroblast growth factor 15 (FGF15) and fibroblast growth factor receptor 4 (FGFR4) (FGF15-β-Klotho-FGFR4 axis) through which BA are able to regulate metabolic pathways is well recognized (33). We understand that FGF15 expression is increased, and CA absorption and serum levels are elevated post-VSG (5, 9), thus this BA-FGF15-FGFR4 pathway may also play a key mechanistic role that requires further investigation. Stimulated in a postprandial state by the intestinal FXR, FGF15 synergizes with SHP and down-regulates BA synthesis (34).

In conclusion, we demonstrated that VSG results in ileal villus proliferation and increased ASBT protein expression, with resultant increased BA reabsorption through the ileum. We further report that the absence of the FXR target SHP results in hepatic inflammation despite

weight loss after murine VSG. Due to the resistance of SHP-KO mice to the hepatic steatosis development we cannot be certain that inflammatory changes observed in SHP-KO mice after VSG are a direct manifestation of NASH. Neither SHP overexpression nor deletion exhibited any significant impact on weight loss and hepatic steatosis resolution post-VSG. Detailed investigation of the intestinal axis of BA signaling will be important to completely understand the metabolism changes observed after VSG. These studies will result in discovery of new potential treatment targets and non-invasive bariatric-mimetic strategies for NAFLD patients.

## Supplementary Material

Refer to Web version on PubMed Central for supplementary material.

## Acknowledgements

RJS receives research support from Ablaris, Johnson and Johnson, Novo Nordisk, and Pfiezer, is a paid speaker for Johnson and Johnson, Merck, Novo Nordisk, and Pfizer, serves as a consultant for Angiogen, Eli Lilly, Johnson and Johnson, Novartis, Novo Nordisk, Takeda and Zafgen, and has equity in Zafgen. RK receives research support from Johnson and Johnson.

This work was supported by NIH DK084310 (RK), U01 DK08505 (RK), and Ethicon Endo-Surgery (RJS, RK), NIH P30 DK078392, NIH DK080440 (LW), VA 1I01BX002634 (LW).

## References

1. Liu Q, Bengmark S, Qu S. The role of hepatic fat accumulation in pathogenesis of non-alcoholic fatty liver disease (NAFLD). Lipids in health and disease. 2010; 9:42. [PubMed: 20426802]
2. Bohinc BN, Diehl AM. Mechanisms of disease progression in NASH: new paradigms. Clinics in liver disease. 2012; 16:549–565. [PubMed: 22824480]
3. Pontiroli AE, Benetti A, Folini L, Merlotti C, Frige F. Other aspects of bariatric surgery: liver steatosis, ferritin and cholesterol metabolism. Nutricion hospitalaria. 2013; 28(Suppl 2):104–108. [PubMed: 23834053]
4. Mottin CC, Moretto M, Padoin AV, Kupski C, Swarowsky AM, Glock L, et al. Histological behavior of hepatic steatosis in morbidly obese patients after weight loss induced by bariatric surgery. Obesity surgery. 2005; 15:788–793. [PubMed: 15978148]
5. Myronovych A, Kirby M, Ryan KK, Zhang W, Jha P, Setchell KD, et al. Vertical sleeve gastrectomy reduces hepatic steatosis while increasing serum bile acids in a weight-loss-independent manner. Obesity. 2013
6. Kohli R, Bradley D, Setchell KD, Eagon JC, Abumrad N, Klein S. Weight loss induced by Roux-en-Y gastric bypass but not laparoscopic adjustable gastric banding increases circulating bile acids. J Clin Endocrinol Metab. 2013; 98:E708–E712. [PubMed: 23457410]
7. Steinert RE, Peterli R, Keller S, Meyer-Gerspach AC, Drewe J, Peters T, et al. Bile acids and gut peptide secretion after bariatric surgery: a 1-year prospective randomized pilot trial. Obesity (Silver Spring). 2013; 21:E660–E668. [PubMed: 23804517]
8. Fuchs C, Claudel T, Trauner M. Bile Acid-mediated control of liver triglycerides. Seminars in liver disease. 2013; 33:330–342. [PubMed: 24222091]
9. Ryan KK, Tremaroli V, Clemmensen C, Kovatcheva-Datchary P, Myronovych A, Karns R, et al. FXR is a molecular target for the effects of vertical sleeve gastrectomy. Nature. 2014
10. Zhang Y, Hagedorn CH, Wang L. Role of nuclear receptor SHP in metabolism and cancer. Biochim Biophys Acta. 2011; 1812:893–908. [PubMed: 20970497]
11. Adorini L, Pruzanski M, Shapiro D. Farnesoid X receptor targeting to treat nonalcoholic steatohepatitis. Drug discovery today. 2012; 17:988–997. [PubMed: 22652341]

12. Calkin AC, Tontonoz P. Transcriptional integration of metabolism by the nuclear sterol-activated receptors LXR and FXR. Nature reviews Molecular cell biology. 2012; 13:213–224. [PubMed: 22414897]
13. Wang L, Lee YK, Bundman D, Han Y, Thevananther S, Kim CS, et al. Redundant pathways for negative feedback regulation of bile acid production. Developmental cell. 2002; 2:721–731. [PubMed: 12062085]
14. Zhang Y, Soto J, Park K, Viswanath G, Kuwada S, Abel ED, et al. Nuclear receptor SHP, a death receptor that targets mitochondria, induces apoptosis and inhibits tumor growth. Molecular and cellular biology. 2010; 30:1341–1356. [PubMed: 20065042]
15. Hagio M, Matsumoto M, Fukushima M, Hara H, Ishizuka S. Improved analysis of bile acids in tissues and intestinal contents of rats using LC/ESI-MS. Journal of lipid research. 2009; 50:173–180. [PubMed: 18772484]
16. Huang J, Iqbal J, Saha PK, Liu J, Chan L, Hussain MM, et al. Molecular characterization of the role of orphan receptor small heterodimer partner in development of fatty liver. Hepatology. 2007; 46:147–157. [PubMed: 17526026]
17. Wang L, Liu J, Saha P, Huang J, Chan L, Spiegelman B, et al. The orphan nuclear receptor SHP regulates PGC-1alpha expression and energy production in brown adipocytes. Cell metabolism. 2005; 2:227–238. [PubMed: 16213225]
18. Bechmann LP, Kocabayoglu P, Sowa JP, Sydor S, Best J, Schlattjan M, et al. Free fatty acids repress small heterodimer partner (SHP) activation and adiponectin counteracts bile acidinduced liver injury in superobese patients with nonalcoholic steatohepatitis. Hepatology. 2013; 57:1394–1406. [PubMed: 23299969]
19. Boulias K, Katrakili N, Bamberg K, Underhill P, Greenfield A, Talianidis I. Regulation of hepatic metabolic pathways by the orphan nuclear receptor SHP. The EMBO journal. 2005; 24:2624–2633. [PubMed: 15973435]
20. Goodwin B, Jones SA, Price RR, Watson MA, McKee DD, Moore LB, et al. A regulatory cascade of the nuclear receptors FXR, SHP-1, and LRH-1 represses bile acid biosynthesis. Molecular cell. 2000; 6:517–526. [PubMed: 11030332]
21. Watanabe M, Houten SM, Wang L, Moschetta A, Mangelsdorf DJ, Heyman RA, et al. Bile acids lower triglyceride levels via a pathway involving FXR, SHP, and SREBP-1c. The Journal of clinical investigation. 2004; 113:1408–1418. [PubMed: 15146238]
22. Wang L, Han Y, Kim CS, Lee YK, Moore DD. Resistance of SHP-null mice to bile acid-induced liver damage. The Journal of biological chemistry. 2003; 278:44475–44481. [PubMed: 12933814]
23. Yang CS, Yuk JM, Kim JJ, Hwang JH, Lee CH, Kim JM, et al. Small heterodimer partner-targeting therapy inhibits systemic inflammatory responses through mitochondrial uncoupling protein 2. PloS one. 2013; 8:e63435. [PubMed: 23704907]
24. Yuk JM, Shin DM, Lee HM, Kim JJ, Kim SW, Jin HS, et al. The orphan nuclear receptor SHP acts as a negative regulator in inflammatory signaling triggered by Toll-like receptors. Nature immunology. 2011; 12:742–751. [PubMed: 21725320]
25. Schiff ER, Small NC, Dietschy JM. Characterization of the kinetics of the passive and active transport mechanisms for bile acid absorption in the small intestine and colon of the rat. The Journal of clinical investigation. 1972; 51:1351–1362. [PubMed: 5024036]
26. Mottino AD, Hoffman T, Dawson PA, Luquita MG, Monti JA, Sanchez Pozzi EJ, et al. Increased expression of ileal apical sodium-dependent bile acid transporter in postpartum rats. Am J Physiol Gastrointest Liver Physiol. 2002; 282:G41–G50. [PubMed: 11751156]
27. Kohli R, Kirby M, Setchell KD, Jha P, Klustaitis K, Woollett LA, et al. Intestinal adaptation after ileal interposition surgery increases bile acid recycling and protects against obesity-related comorbidities. Am J Physiol Gastrointest Liver Physiol. 2010; 299:G652–G660. [PubMed: 20595624]
28. Kohli R, Setchell KD, Kirby M, Myronovych A, Ryan KK, Ibrahim SH, et al. A surgical model in male obese rats uncovers protective effects of bile acids post-bariatric surgery. Endocrinology. 2013; 154:2341–2351. [PubMed: 23592746]
29. Habegger KM, Al-Massadi O, Heppner KM, Myronovych A, Holland J, Berger J, et al. Duodenal nutrient exclusion improves metabolic syndrome and stimulates villus hyperplasia. Gut. 2013

30. Perkins WJ, Hale ER, Fernandez AZ, Dawson P, Weinberg RB. Mo2046 Differential Effects of Laparoscopic Sleeve Gastrectomy and Roux-en-Y Gastric Bypass on Dietary Fatty Acid Absorption, Bile Acid Absorption, and Post-Prandial Gut Hormone Secretion. Gastroenterology. 2014; 146:S-726–S-727.

31. Kang K, Schmahl J, Lee JM, Garcia K, Patil K, Chen A, et al. Mouse ghrelin-O-acyltransferase (GOAT) plays a critical role in bile acid reabsorption. FASEB journal : official publication of the Federation of American Societies for Experimental Biology. 2012; 26:259–271. [PubMed: 21965605]

32. Vos TA, Ros JE, Havinga R, Moshage H, Kuipers F, Jansen PL, et al. Regulation of hepatic transport systems involved in bile secretion during liver regeneration in rats. Hepatology. 1999; 29:1833–1839. [PubMed: 10347127]

33. Kir S, Kliewer SA, Mangelsdorf DJ. Roles of FGF19 in liver metabolism. Cold Spring Harbor symposia on quantitative biology. 2011; 76:139–144. [PubMed: 21813638]

34. Inagaki T, Choi M, Moschetta A, Peng L, Cummins CL, McDonald JG, et al. Fibroblast growth factor 15 functions as an enterohepatic signal to regulate bile acid homeostasis. Cell metabolism. 2005; 2:217–225. [PubMed: 16213224]

**What is already known about this subject**

- Nonalcoholic fatty liver disease (NAFLD) is characterized with the lipid accumulation in the liver and its severe form nonalcoholic steatohepatitis (NASH) is manifested with hepatic damage and inflammation.
- Bariatric surgery is an effective method of treatment of metabolic syndrome, including its comorbidity NAFLD, which is accompanied by the elevation of serum bile acid levels.
- Transcription factor farnesoid-X receptor (FXR) is an important bile acid target which is responsible for the body weight reduction and glucose tolerance improvement after vertical sleeve gastrectomy (VSG).

**What this study adds to the literature**

- Bile acid absorption area is increased in mice after VSG due to the terminal ileum villi elongation and increased active surface of the ileal apical sodium-dependent bile acid transporter protein (ASBT).
- Reduction of body weight, hepatic steatosis in mice post-VSG is independent of the FXR target - small heterodimer partner (SHP).
- The absence of SHP produces hepatic inflammation after VSG that develops despite weight loss.

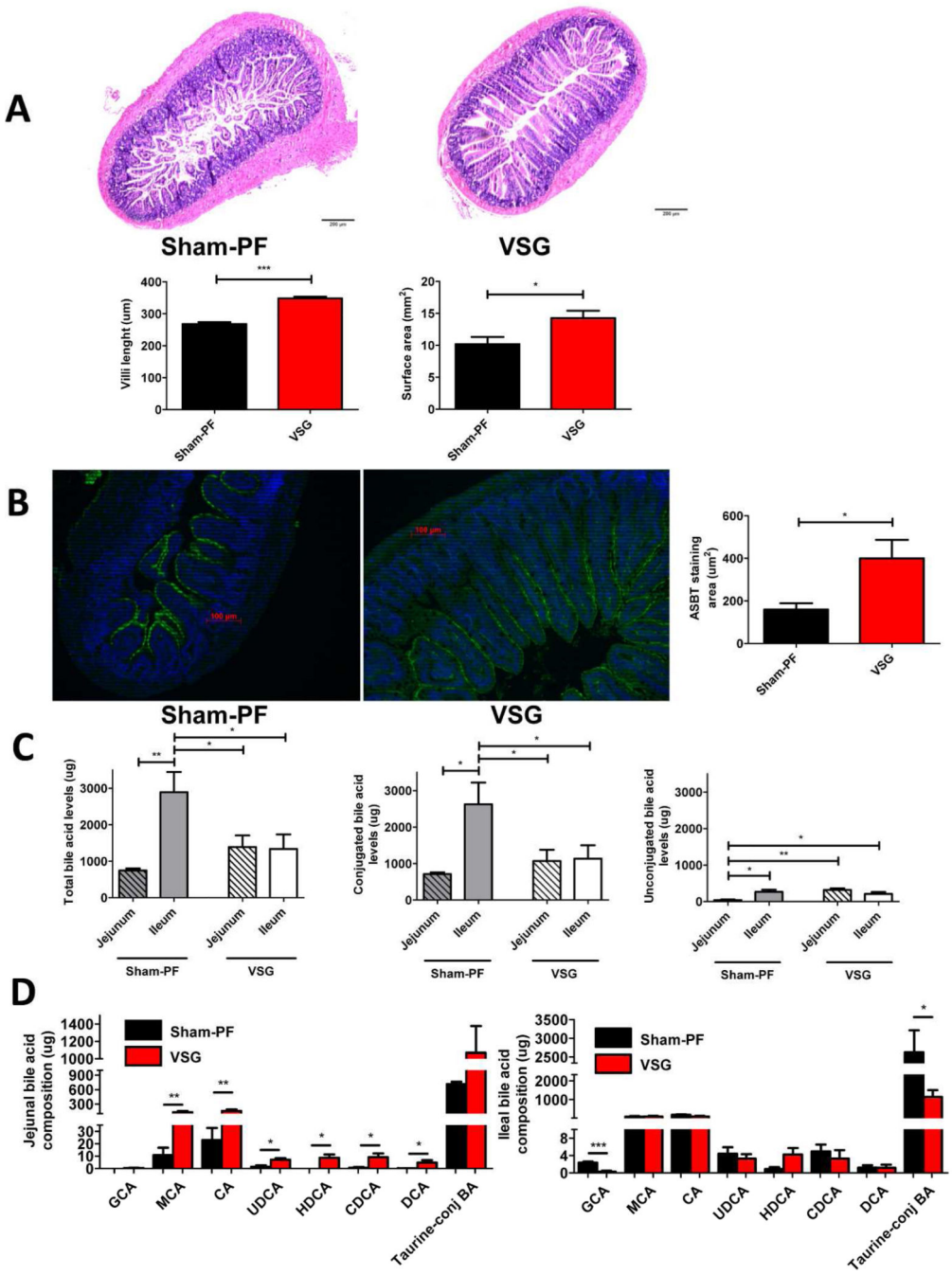


**Figure 1.**

**A. Hematoxylin & eosin staining and villi characteristics of the terminal ileum sections obtained from the Sham-PF and VSG mice 60 days post-surgery**.

Villi in VSG mice were much longer (***=p <0.0001, t-test) and had greater surface area (*=p <0.05, t-test) compared to Sham-PF mice. N: VSG=28, Sham-PF=26.

**B. ASBT staining of the terminal ileum sections and stained surface area of Sham-PF and VSG mice 60 days post-surgery**.

Representative 20× magnification terminal ileum sections stained with ASBT antibody (green). Stained area was significantly larger in VSG compared to Sham-PF mice. N: VSG=5, Sham-PF=5. (*=p <0.05, t-test).

**C. The levels of total, conjugated and unconjugated BA in the jejunum and ileum of Sham-PF and VSG mice 60 days post-surgery**.

Total and conjugated BA levels were significantly higher in the ileum of Sham-PF mice compared to the jejunum of Sham-PF and jejunum and ileum of VSG mice. Unconjugated BA levels were the lowest in the jejunum of Sham-PF mice. N: VSG=5, Sham-PF=5. (*=p <0.05, **=p<0.01, one-way ANOVA and t-test).

**D. Intestinal BA composition analysis in the jejunum and ileum of Sham-PF and VSG mice 60 days post-surgery**.

Muricholic, cholic, ursodeoxycholic, hyodeoxycholic, chenodeoxycholic and deoxycholic acid levels were significantly higher in the jejunum of VSG mice. N: VSG=5, Sham-PF=5. (*=p<0.05, **=p<0.01, t-test). The levels of these acids were not different between both groups in the ileum but taurine-conjugated BA levels were higher in the Sham-PF compared to the VSG mice (*=p<0.05, t-test). The following BA are indicated: glycocholic acid (GCA), muricholic acid (MCA), cholic acid (CA), ursodeoxycholic acid (UDCA), hyodeoxycholic acid (HDCA), chenodeoxycholic acid (CDCA), deoxycholic acid (DCA).

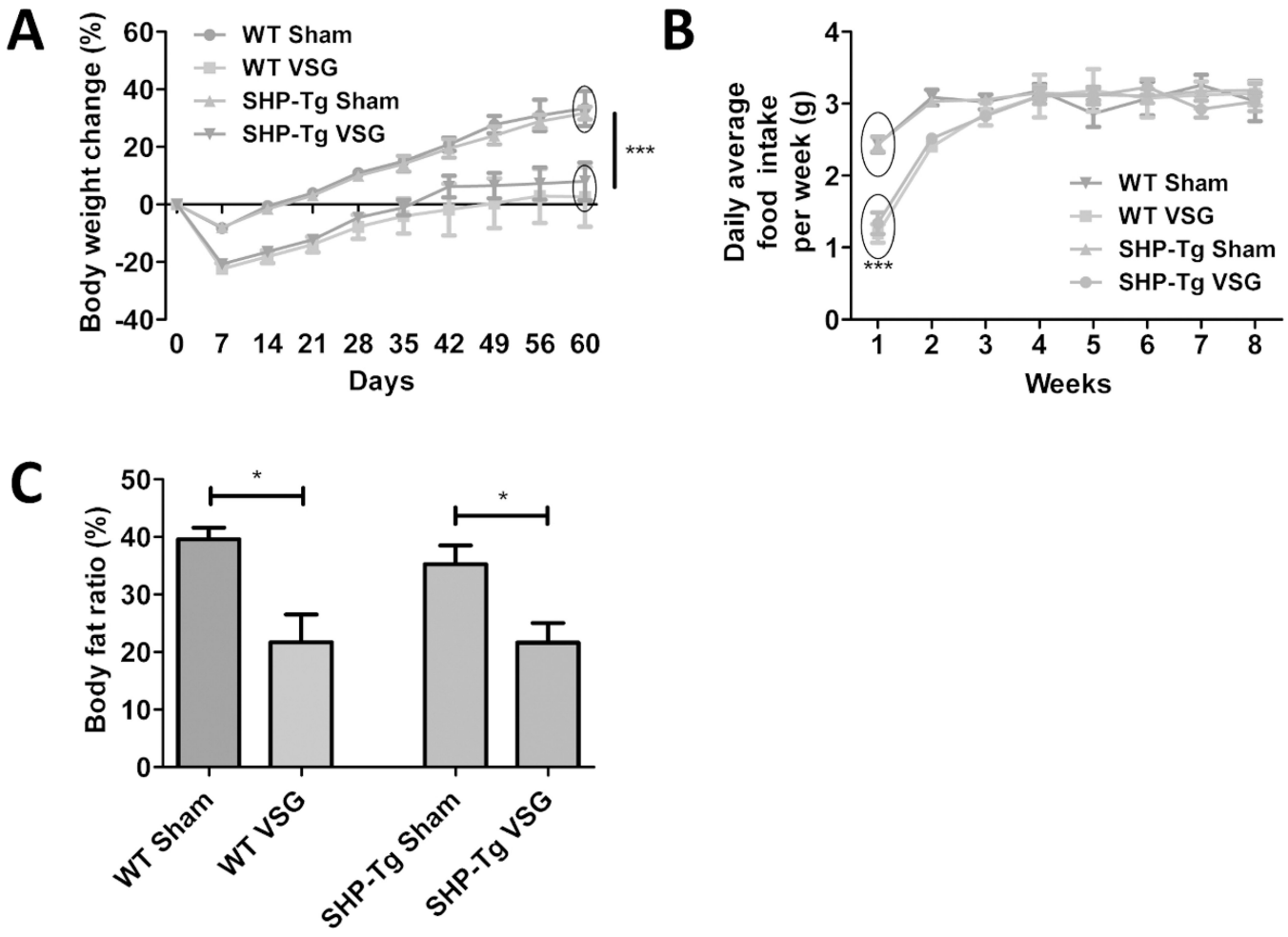


**Figure 2.**

**A. Body weight change over the 60 days post-surgery period in WT Sham, WT VSG, SHP-Tg Sham and SHP-Tg VSG groups**.

Both VSG groups lost more weight post-surgery and gained significantly less compared to Sham groups. No difference was observed between SHP-Tg VSG and WT VSG mice in terms of body weight gain post-surgery. N: WT Sham=5, WT VSG= 6, SHP-Tg Sham=6, SHP-Tg VSG =7. (***=$p<0.0001$, two-way ANOVA).

**B. Daily average food intake per week**.

VSG groups consumed less food compared to Sham groups only during the first week post-surgery. N: WT Sham=5, WT VSG= 6, SHP-Tg Sham=6, SHP-Tg VSG =7. (***=$p<0.0001$, two-way ANOVA).

**C. Body fat ratio at 49 days post-surgery**.

Body fat ratio was lower in both VSG groups compared to their respective Sham groups. This parameter was not different between SHP-Tg VSG and WT VSG mice. N: WT Sham=5, WT VSG= 6, SHP-Tg Sham=6, SHP-Tg VSG =7. (*=$p<0.05$, one-way ANOVA).

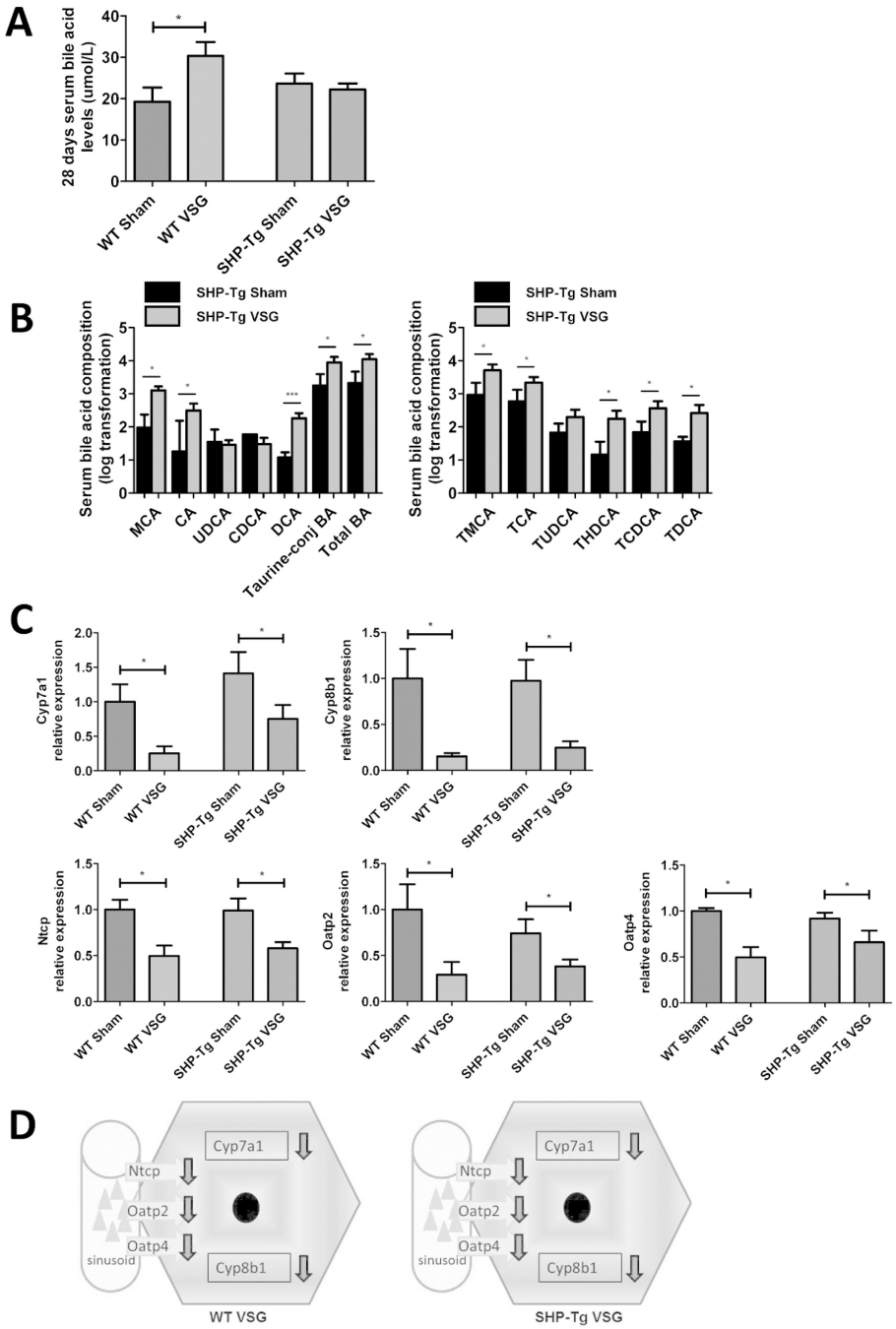


**Figure 3.**

**A. Fasting serum total BA levels at day 28 post-surgery**.

Serum BA levels were higher in WT VSG group compared to WT Sham group, however, in SHP-Tg VSG mice they remained at the same level as in SHP-Tg Sham mice at this time-point. N: WT Sham=5, WT VSG= 6, SHP-Tg Sham=6, SHP-Tg VSG =7. (*=p<0.05, one-way ANOVA).

**B. Serum BA composition analysis of SHP-Tg Sham and SHP-Tg VSG mice at day 60 post-surgery: unconjugated, total taurine-conjugated and total BA levels (left) and individual taurine-conjugated BA levels (right)**.

The majority of BA and, as a result, total BA levels, were significantly higher in serum of SHP-Tg VSG compared to SHP-Tg Sham mice. The following BA are indicated: muricholic acid (MCA), cholic acid (CA), ursodeoxycholate (UDCA), chenodeoxycholate (CDCA), deoxycholate (DCA), tauromuricholate (TMCA), taurocholate (TCA), tauroursodeoxycholate (TUDCA), taurohyodeoxycholate (THDCA), taurochenodeoxycholate (TCDCA), taurodeoxycholate (TDCA). N: SHP-Tg Sham=6, SHP-Tg VSG =7. *=$p<0.05$, ***=$p<0.0001$, t-test).

**C. Hepatic BA synthesis and uptake gene expression at day 60 post-surgery**.

mRNA levels of the genes coding for the BA production (Cyp7a1 and Cyp8b1) and BA uptake (Ntcp, Oatp2 and Oatp4) were measured by RT-PCR and expressed in relative expression units. All these genes were significantly down-regulated in VSG mice with normal or increased hepatic SHP expression. N: WT Sham=4, WT VSG= 5, SHP-Tg Sham=4, SHP-Tg VSG =6. (*=$p<0.05$, one-way ANOVA, t-test).

**D. Scheme of hepatic BA synthesis and uptake gene expression in WT and SHP-Tg mice post-VSG**.

BA production and import were similarly down-regulated in both WT and SHP-Tg mice 60 days after VSG.

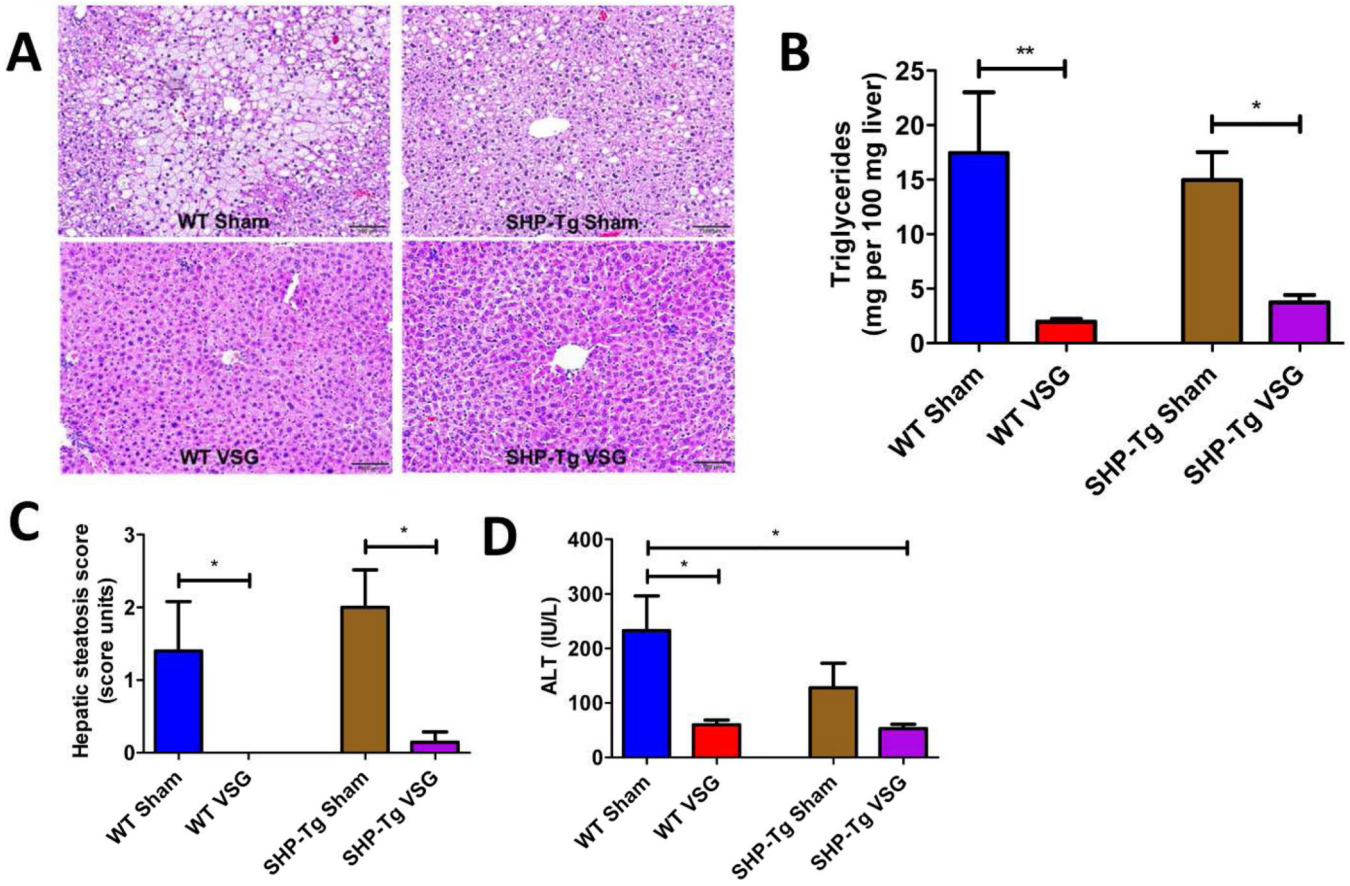


**Figure 4.**

**A. Liver histology 60 days post-surgery**.

Representative 20× magnification hematoxylin-eosin stained sections showed massive fat accumulation in the livers of both Sham groups' mice, while both SHP-Tg VSG and WT VSG mice had normal hepatic microstructure.

**B. Hepatic triglyceride content 60 days post-surgery**.

Liver triglyceride levels were lower in SHP-Tg VSG and WT VSG mice compared to their Sham controls. The levels were not statistically different between both VSG groups. N: WT Sham=5, WT VSG= 6, SHP-Tg Sham=6, SHP-Tg VSG =7. (*=p<0.05, **=p<0.01, one-way ANOVA).

**C. Hepatic steatosis score 60 days post-surgery**.

Hepatic steatosis score was improved in both WT and SHP-Tg mice after VSG. N: WT Sham=5, WT VSG= 6, SHP-Tg Sham=6, SHP-Tg VSG =7. (*=p<0.05, one-way ANOVA).

**D. Plasma ALT levels 60 days post-surgery**.

ALT levels were lower in WT VSG and SHP-Tg VSG groups compared to WT Sham group. N: WT Sham=5, WT VSG= 6, SHP-Tg Sham=6, SHP-Tg VSG =7. (*=p<0.05, one-way ANOVA, t-test).

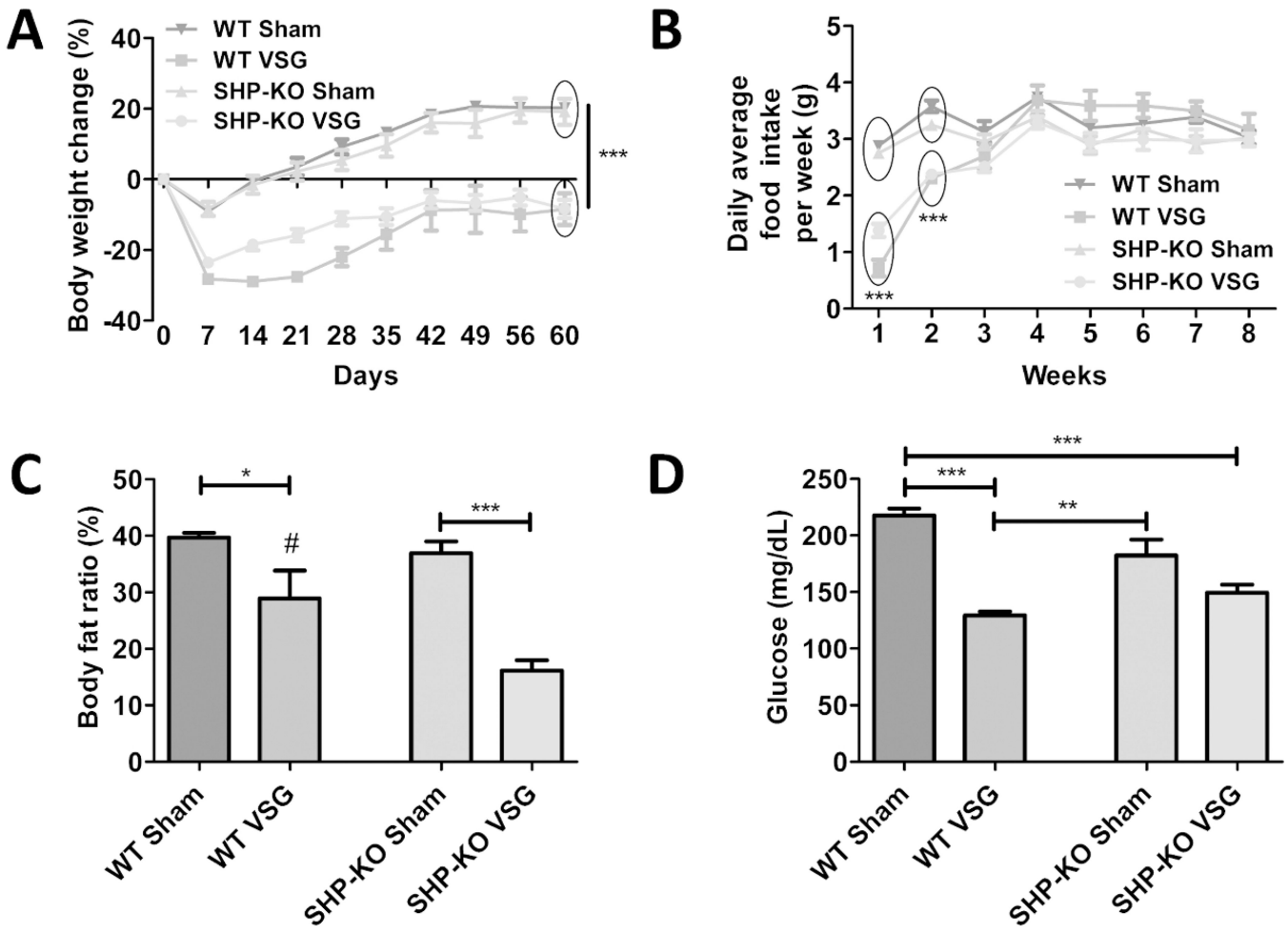


**Figure 5.**

**A. Body weight change over the 60 days post-surgery period in WT Sham, WT VSG, SHP-KO Sham and SHP-KO VSG groups**.

Both VSG groups lost more weight and starting from day 5 post-surgery until the end of experiment gained significantly less compared to Sham groups. No difference was observed between SHP-KO VSG and WT VSG mice in terms of body weight gain post-surgery. N: WT Sham=4, WT VSG= 4, SHP-KO Sham=5, SHP-KO VSG =8. (***=p<0.0001, two-way ANOVA).

**B. Daily average food intake per week**.

Both VSG groups had reduced food intake up to two weeks post-surgery compared to Sham groups but no difference was observed thereafter. N: WT Sham=4, WT VSG= 4, SHP-KO Sham=5, SHP-KO VSG =8. (***=p<0.0001, two-way ANOVA).

**C. Body fat ratio at 49 days post-surgery**.

Body fat ratio was lower in VSG groups compared to their respective Sham groups. Additionally, fat ratio was much lower in SHP-KO VSG compared to WT VSG mice. N: WT Sham=4, WT VSG= 4, SHP-KO Sham=5, SHP-KO VSG =8. (*=p<0.05, ***=p<0.0001, #=p<0.05 WT VSG vs. SHP-KO VSG, one-way ANOVA).

**D. Fasting serum glucose levels 14 days post-surgery**.

Serum glucose levels were significantly lower in WT VSG group compared to both WT Sham and SHP-KO Sham groups, while in SHP-KO VSG mice these levels were not statistically different compared to SHP-KO Sham group. N: WT Sham=4, WT VSG= 4, SHP-KO Sham=5, SHP-KO VSG =8. (**=p<0.01, ***=p<0.0001, one-way ANOVA).

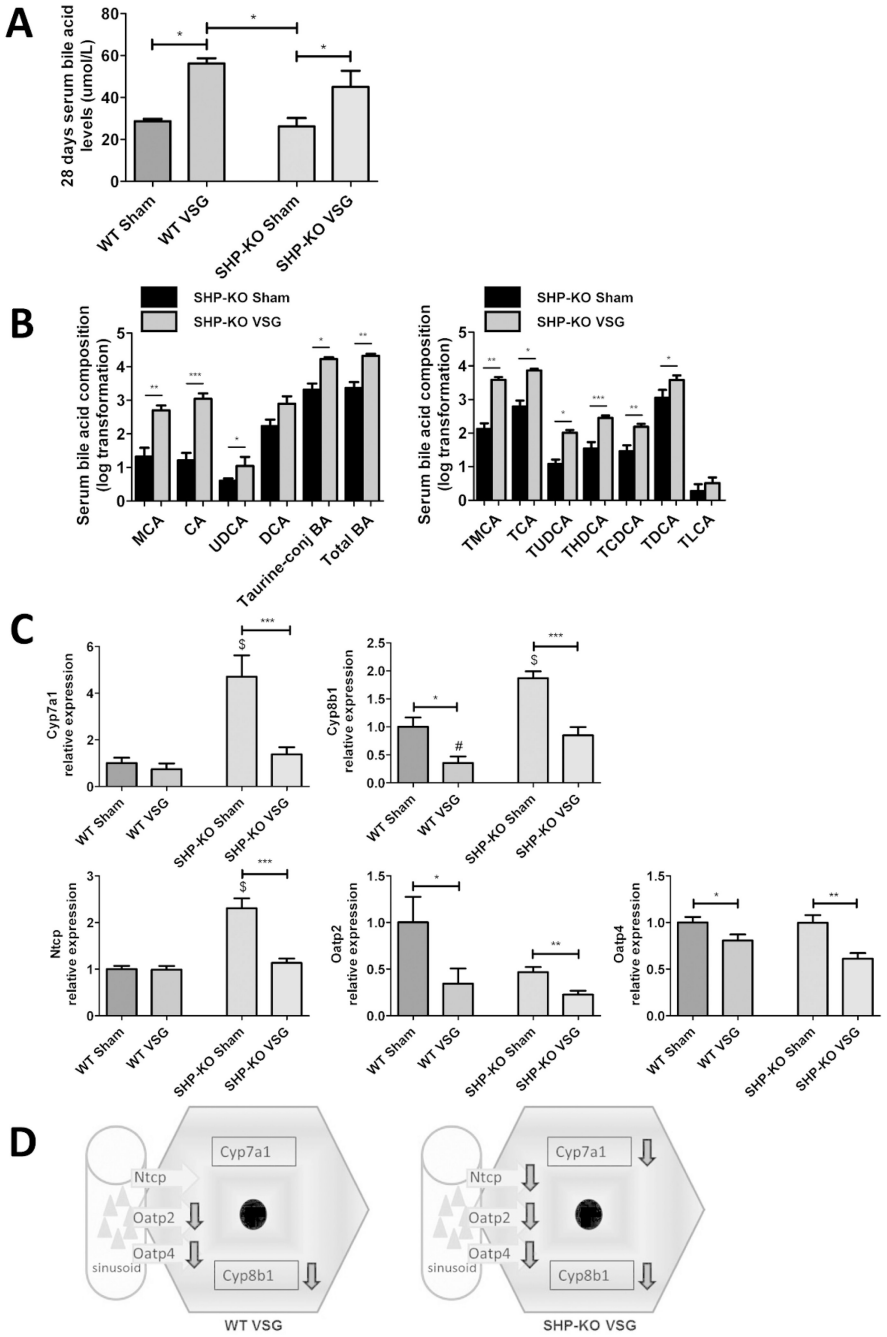


**Figure 6.**

**A. Fasting serum total BA levels at day 28 post-surgery**.

Serum BA levels were higher in both VSG groups compared to Sham groups. N: WT Sham=4, WT VSG= 4, SHP-KO Sham=5, SHP-KO VSG =8. (*=p<0.05, one-way ANOVA, t-test).

**B. Serum BA composition analysis of SHP-KO Sham and SHP-KO VSG mice at day 60 post-surgery: unconjugated, total taurine-conjugated and total BA levels (left) and individual taurine-conjugated BA levels (right)**.

The majority of BA levels and, as a result, total BA levels, were significantly higher in serum of SHP-KO VSG compared to SHP-KO Sham mice. The following BA are indicated: muricholic acid (MCA), cholic acid (CA), ursodeoxycholate (UDCA), deoxycholate (DCA), tauromuricholate (TMCA), taurocholate (TCA), tauroursodeoxycholate (TUDCA), taurohyodeoxycholate (THDCA), taurochenodeoxycholate (TCDCA), taurodeoxycholate (TDCA), taurolithocholate (TLCA). N: SHP-KO Sham=5, SHP-KO VSG =8. *=p<0.05, **=p<0.01, ***=p<0.0001, t-test).

**C. Hepatic BA synthesis and uptake gene expression at day 60 post-surgery**.

mRNA levels of the genes coding for the BA production (Cyp7a1 and Cyp8b1) and BA uptake (Ntcp, Oatp2 and Oatp4) were measured by RT-PCR and expressed in relative expression units. Being predominantly higher in SHP-KO Sham mice, these BA synthesis and hepatocyte import genes, were significantly down-regulated in both VSG groups. N: WT Sham=4, WT VSG= 4, SHP-KO Sham=5, SHP-KO VSG =7. (*=p<0.05, **=p<0.01, ***=p<0.0001, $=p<0.0001 SHP-KO Sham vs. WT Sham and WT VSG, #=p<0.05 WT VSG vs. SHP-KO VSG, one-way ANOVA, t-test).

**D. Scheme of hepatic BA synthesis and uptake gene expression in WT and SHP-KO mice post-VSG**.

BA production and import were similarly down-regulated in both WT and SHP-KO mice 60 days after VSG.

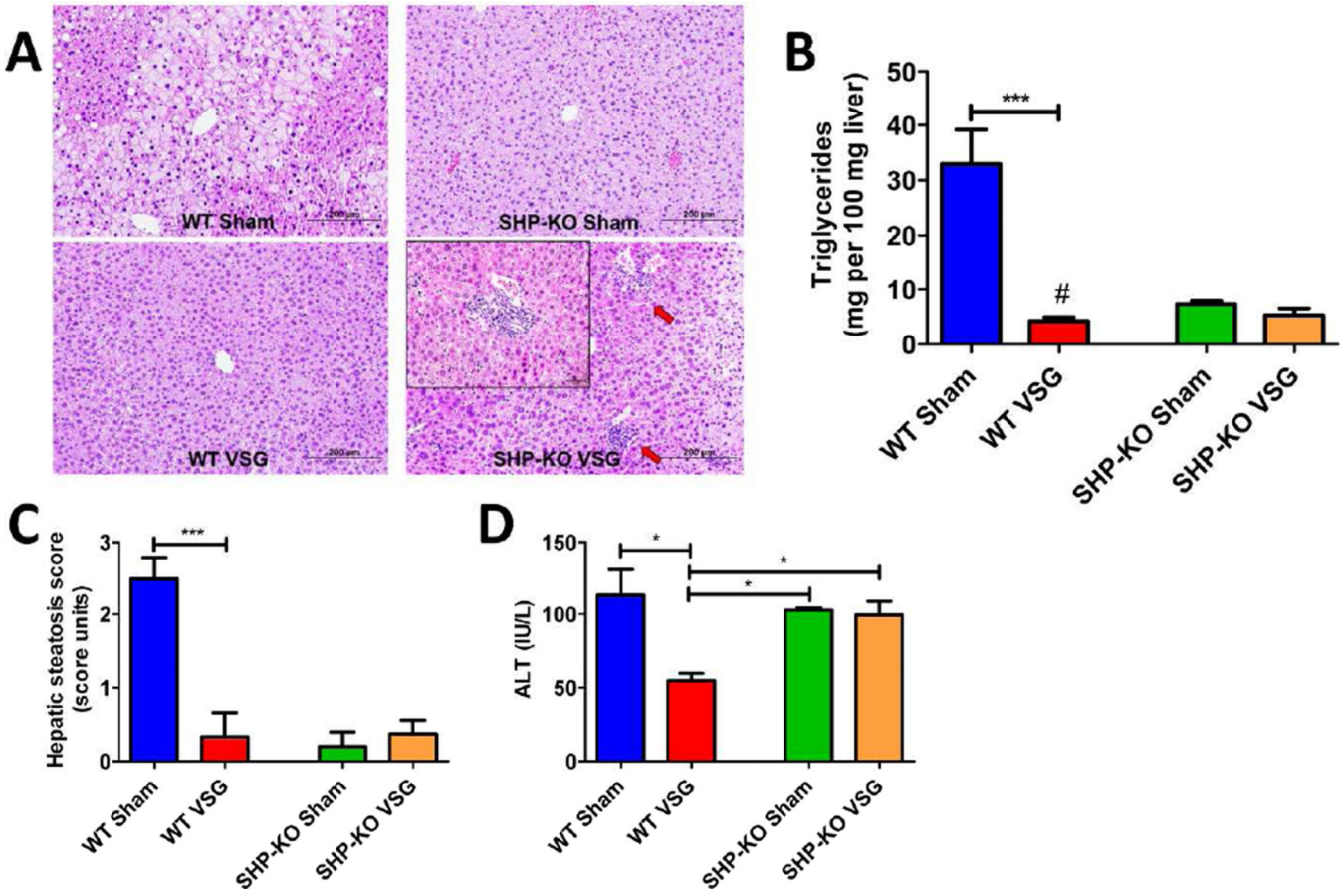


**Figure 7.**

**A. Liver histology 60 days post-surgery**.

Representative 20× magnification hematoxylin-eosin stained sections show massive fat accumulation in the livers of WT Sham mice while no pathological changes were observed in case of WT VSG mice. Both SHP-KO groups showed low liver lipid accumulation but multiple areas of neutrophil infiltration were present in the livers of SHP-KO VSG mice. Arrows show areas of neutrophil infiltration. 40× magnification image with massive neutrophil infiltration in the liver is shown in the upper left corner of SHP-KO VSG section.

**B. Hepatic triglyceride content 60 days post-surgery**.

Liver triglyceride levels were the lowest in WT VSG mice with significance compared to WT Sham and SHP-KO Sham mice. However, hepatic triglycerides were not significantly different between SHP-KO VSG and SHP-KO Sham mice. N: WT Sham=4, WT VSG= 4, SHP-KO Sham=5, SHP-KO VSG =8. ***=$p<0.0001$, #=$p<0.05$ WT VSG vs. SHP-KO Sham, one-way ANOVA, t-test).

**C. Hepatic steatosis score 60 days post-surgery**.

Hepatic steatosis score was improved in WT mice after VSG, however, no difference was observed between SHP-KO Sham and SHP-KO VSG mice. N: WT Sham=4, WT VSG= 4, SHP-KO Sham=5, SHP-KO VSG =8. (***=$p<0.0001$, one-way ANOVA).

**D. Plasma ALT levels 60 days post-surgery**.

ALT levels were the lowest in WT VSG group compared to WT Sham, SHP-KO Sham and SHP-KO VSG groups. (*=$p<0.05$, one-way ANOVA).